Safe Reference Following on the Inverted Pendulum

Åkesson, Johan

1999

[Link to publication](#)

Total number of authors:
1

Safe Reference Following on the Inverted Pendulum

Johan Åkesson

Department of Automatic Control	Document name
Lund Institute of Technology	INTERNAL REPORT
Box 118	Date of issue
SE-221 00 Lund Sweden	August 1999
	Document Number
	ISRN LUTFD2/TFRT--7587--SE

Author(s)	Supervisor
Johan Åkesson	Karl Johan Åström
	Sponsoring organisation

Title and subtitle
Safe Reference Following on the Inverted Pendulum

Abstract

This work discusses methods to obtain reference following on unstable systems. The task is critical; introduction of refernce signal might cause instability in some cases. It is thus interesting to develop strategies that offer acceptable reference following, but also guarantees stability. In practice similiar problems arises in flight control systems for unstable fighter aircrafts.

Experimental verifications of the discussed strategies have been carried out on a Furuta pendulum, i.e. an inverted pendulum. The system is ustable and thus well suited for the task. A few different strategies for achieving have been examined and experimentally evaluated.

Key words
Inverted Pendulum, Manual Control

Classification system and/or index terms (if any)

Supplementary bibliographical information

ISSN and key title		*ISBN*
0280–5316		

Language	*Number of pages*	*Recipient's notes*
English	26	
Security classification		

Contents

Figure 1   An illustration of the problem formulation dealt with in this work.

1. Introduction

This report deals with manual control of an unstable system with actuator saturation. The control task is critical, the manual control must not be performed in such way that it causes instability. Typically this problem arises when the process has limitations on the control signal, i.e saturation and / or rate limits. The available control authority is thus limited and must be shared between stabilization and manual control.

Examples of manual control of unstable systems in practise are modern fighter aircrafts, e.g JAS 39 Gripen. The aircraft is unstable and has to be stabilized by the control system in order to operate. The problem here is the rate limited control servos, that may reduce the stability drastically when saturated. This issue is discussed further in Rundqwist *et al.* (1997).

1.1 Problem Formulation

Our problem formulation can be illustrated as in fig 1. The process to be controlled is unstable, and the control signal is restricted by saturation which is the basic problem in our set up. Further, we have two objectives, possibly conflicting, for the controller. The first and most important is to guarantee stability of the process. This issue should always be given the highest priority. The second objective is to perform manual control of a certain state of the process, e.g position or velocity. This introduction of reference signal may lead to violation of the stabilization condition if the authority of this control task is not limited. Strategies to achieve "good" reference following (the meaning of "good" is discussed in section 3.2) with guaranteed stability is thus the main subject of this work.

1.2 Experiments

This work focuses on experiments. Desirable is an unstable process that is fairly simple to use and calculate controllers for. We would like to concentrate on evaluation of different control strategies. The process used is an inverted pendulum. In our implementation, the pendulum is attached to a rotating arm instead of the classic linear cart, see fig 2. This is a nice property since there are no end points, which is an advantage, for example when velocity control is performed. The pendulum may seem far apart from an complex fighter aircraft, but it has the capital similiarity of beeing unstable. Thus, the inverted pendulum serves as a suitable process for our purposes.

The control task is to control the velocity of the pivot point for the pendulum, this is the controlled state, but not in a way that violates the stabilization condition. As discussed earlier, the problem is that the control
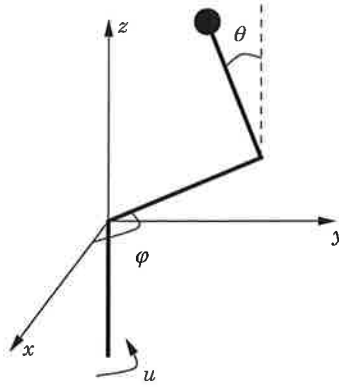
Figure 2 A schematic picture of the Furuta pendulum

authority is limited, i.e there is a saturation on the process input. The consequences of this is investigated in Brufani (1997). In order to guarantee sufficient authority to the stabilizing control, restrictions on the reference has to be made.

1.3 Roadmap

A detailed description of the inverted pendulum is given in section 2. A stabilizing control law is derived. This section also discusses the issues swing up of the pendulum and friction compensation. This sections are less relevant for the solution of the manual control problem and may be skipped, but they are indeed recommended for the interested reader.

In section 3 the problem formulation and different strategies is discussed. A few quantitative measures of control performance is given in 3.2. A heuristic approach based on rate limiters is given in section 3.3, while the strategy presented in Brufani (1997) is implemented and evaluated in section 3.4. A description of the experimental set up is given in section 4, which also contains a report of experienced problems during the project. In appendix A the user interface is described. This section serves as a brief user manual for the control application used for the experiments.

2. The Furuta Pendulum

In this section a mathematical model for the Furuta pendulum which was used in the experiments is presented. The model is based on the derivation in Gäfvert (1998), only the results are given here.

Consider the Furuta pendulum in fig 2. Let the length of the pendulum be l, the mass of the weight M, the mass of the pendulum m, its moment of inertia J and the moment of inertia for the arm J_p. The length of the arm is r. The angle of the pendulum, θ, is defined to be zero when in upright position and positive when the pendulum is moving clockwise. The angle of the arm, φ is positive when the arm is moving in counter clockwise direction. Further, the central vertical axis is connected to a DC motor which adds a torque proportional to the control signal u.

6

2.1 Mathematical model

The complete derivation of the Furuta pendulum dynamics is excluded here. The derivation is based on Lagrange theory and can be read in Gäfvert (1998).

Using the definitions made above, the equations of motion can be written

$$(J_p + Ml^2)(\ddot{\theta} - \dot{\varphi}^2 \sin\theta \cos\theta) + Mrl\ddot{\varphi}\cos\theta - gl(M + m/2)\sin\theta = 0$$
$$Mrl\ddot{\theta}\cos\theta - Mrl\dot{\theta}^2 \sin\theta + 2(J_p + ml^2)\dot{\theta}\dot{\varphi}\sin\theta\cos\theta \qquad (1)$$
$$+(J + mr^2 + Mr^2 + (J_p + ml^2)\sin^2\theta)\ddot{\varphi} = u$$

Introduce

$$\alpha = J_p + Ml^2 \quad \beta = J + Mr^2 + mr^2$$
$$\gamma = Mrl \qquad \varepsilon = lg(M + m/2)$$

and the equations of motion can be rewritten:

$$\alpha\ddot{\theta} - \alpha\dot{\varphi}^2 \sin\theta\cos\theta + \gamma\ddot{\varphi}\cos\theta - \varepsilon\sin\theta = 0$$
$$\gamma\ddot{\theta}\cos\theta - \gamma\dot{\theta}^2 \sin\theta + 2\alpha\dot{\theta}\dot{\varphi}\sin\theta\cos\theta + (\beta + \alpha\sin^2\theta)\ddot{\varphi} = u \qquad (2)$$

The coefficients for the pendulum used in the experiments are (see Svensson (1998)):

$$l = 0.413m \qquad r = 0.235m$$
$$M = 0.01kg \qquad J = 0.05kgm^2$$
$$J_p = 0.0009kgm^2 \quad m = 0.02kg$$

This model was used for further calculations and simulation.

2.2 Stabilization of the pendulum

Our first objective before manual control can be performed is to stabilize the pendulum in upright position. Notice, that the angular velocity of the arm is taken into account when the linearization is made. This is because our objective is to perform velocity control, and gain scheduling will be used to modify the control law with varying velocity. This means that the controller will not be linear, it will change with varying arm velocity.

Since all states is measurable, linear state feedback is used. The method is simple and allow arbitrary placement of the closed loop poles. It is then necessary to derive a linear model of the pendulum. Introduce the state vector

$$x = \begin{pmatrix} \theta & \dot{\theta} & \varphi & \dot{\varphi} \end{pmatrix}^T$$

and linearization of the system (2) around

$$x = \begin{pmatrix} 0 & 0 & 0 & \dot{\varphi}_0 \end{pmatrix}^T$$

gives

$$\dot{x} = Ax + Bu = \begin{pmatrix} 0 & 1 & 0 & 0 \\ \frac{\alpha\beta\dot{\varphi}_0^2 + \beta\varepsilon}{\alpha\beta - \gamma^2} & 0 & 0 & 0 \\ 0 & 0 & 0 & 1 \\ \frac{-\alpha\gamma\dot{\varphi}_0^2 - \gamma\varepsilon}{\alpha\beta - \gamma^2} & 0 & 0 & 0 \end{pmatrix} x + \begin{pmatrix} 0 \\ \frac{-\gamma}{\alpha\beta - \gamma^2} \\ 0 \\ \frac{\alpha}{\alpha\beta - \gamma^2} \end{pmatrix} u \qquad (3)$$

The control law can be written

$$u = Lx \qquad (4)$$

where

$$L = \begin{pmatrix} l_1 & l_2 & l_3 & l_4 \end{pmatrix}$$

The control law (4) applied on the system (3) gives the closed loop dynamics

$$\dot{x} = (A - BL)x$$

The characteristic polynomial of the closed loop system is

$$s^4 + \frac{\alpha l_4 - \gamma l_2}{\alpha\beta - \gamma^2}s^3 + \frac{\alpha l_3 - \beta\varepsilon - \alpha\beta\dot{\varphi}_0^2 - \gamma l_1}{\alpha\beta - \gamma^2}s^2 - \frac{(\alpha\dot{\varphi}_0^2 + \varepsilon)l_4}{\alpha\beta - \gamma^2}s - \frac{(\alpha\dot{\varphi}_0^2 + \varepsilon)l_3}{\alpha\beta - \gamma^2}$$

Let desired characteristic polynomial for the closed loop system be

$$(s^2 + 2\omega_1\zeta_1 + \omega_1^2)(s^2 + 2\omega_2\zeta_2 + \omega_2^2)$$

Identification of coefficients gives

$$l_1 = -\frac{\alpha\beta\dot{\varphi}_0^2 + \beta\varepsilon}{\gamma} - \frac{\alpha\beta - \gamma^2}{\gamma}\left(\frac{\alpha}{\alpha\dot{\varphi}_0^2 + \varepsilon}\omega_1^2\omega_2^2 + \omega_1^2 + 4\zeta_1\zeta_2\omega_1\omega_2 + \omega_2^2\right)$$

$$l_2 = -\frac{\alpha\beta - \gamma^2}{\gamma}\left(\frac{2\alpha}{\alpha\dot{\varphi}_0^2 + \varepsilon}(\zeta_2\omega_1^2\omega_2 + \zeta_1\omega_2^2\omega_1) + 2\zeta_1\omega_1 + 2\zeta_2\omega_2\right)$$

$$l_3 = -\frac{\alpha\beta - \gamma^2}{\alpha\dot{\varphi}_0^2 + \varepsilon}\omega_1^2\omega_2^2$$

$$l_4 = -\frac{\alpha\beta - \gamma^2}{\alpha\dot{\varphi}_0^2 + \varepsilon}(2\zeta_2\omega_1^2\omega_2 + 2\zeta_1\omega_2^2\omega_1)$$

For the experiments presented in this work, the following parameters were used:

$$\omega_1 = \omega_2 = 8.5$$
$$\zeta_1 = \zeta_2 = 0.9$$

An important observation concerning the closed loop system can be made. If the transfer function from u to φ is examined, zeros appear at

$$z = \pm\sqrt{\frac{a_{12}b_{12}a_{14} - a_{12}b_{14}}{b_{14}}}$$

(coefficients from the system matrices) which is, one zero on the positive real axis. This corresponds to a non minimum phase system and will limit the achievable control performance.

2.3 Swing Up

An issue that has not so much to do with the main problem of manual control is swinging up the pendulum from rest to upright position. Never the less it is a practical feature to implement, and a nice feature for a demonstration. A brief description of a swing up strategy will be presented, interested readers are encouraged to consult Åström and Furuta (1999)

In this section a simplified model of the pendulum will be used. Instead of the Furuta pendulum a pendulum attached to a linear cart is modeled. The reason for this is that the calculations will be significantly easier and the model will still be sufficiently accurate for our purposes. Using the same terminology as above, the equations of motion may be written

$$J_p \frac{d^2\theta}{dt} = Mgl\sin\theta - Mla\cos\theta$$
$$\frac{d^2\varphi}{dt^2} = a$$

(5)

where a is the applied acceleration.

Introducing the normalizations

$$\omega_0 = \sqrt{\frac{Mgl}{J_p}} \quad u = \frac{a}{g}$$

the equations of motion may be rewritten as

$$\frac{d^2\theta}{dt} = \omega_0^2 \sin\theta - \omega_0^2 u \cos\theta$$
$$\frac{d^2\varphi}{dt} = ug$$

Swing Up by Energy Control   The strategy used is based on energy control and is presented in Åström and Furuta (1999). The basic idea is to pump energy into the system, so that it finally contains enough energy to pass the upright equibrillium. Well there, switching to a control law that catches and stabilizes the pendulum is performed.

The energy of the uncontrolled pendulum, using the same terminology as above, may be expressed as

$$E_n = \frac{E}{Mgl} = \frac{\dot{\theta}^2}{2\omega_0^2} + \cos\theta - 1$$

The energy is thus zero when the pendulum is at rest in upright position. The energy is normalized with respect to Mgl.

A control law proposed in Åström and Furuta (1999) is

$$u = sat(k(E_n - E_0)sign(\dot{\theta}\cos\theta))$$

E_0 is here the desired energy of the system, i.e zero. The design parameters for this method is k and the saturation limits. In our implementation k was

set to 100 and the saturation limits to ±1. This control law performs the desired swing up.

The control law presented above perform a swing up that makes the pendulum pass the upright equibrillium. However, it remains to catch and stabilize the pendulum. This is done by switching from the swing up control law to a catch control law and finally to a stabilizing control law. LQ theory is used for calculation of the catching controller. Large punishments on the states θ and $\dot{\theta}$ and a smaller punishment on $\dot{\varphi}$ gives a LQ controller with the desired properties. When the pendulum i catched, switching to the stabilizing controller is performed.

A Nonlinear Observer   In order to implement the swing up strategy measures of θ and $\dot{\theta}$ is needed. This is a problem since both this signals are discontinues at a certain angle. The measurement of θ exhibits a step form 0 to 2π at this angle, which can be dealt with by adding an offset to the measured signal. $\dot{\theta}$ however exhibits more serious discontinuesies and we have therefor chosen to use a nonlinear observer presented in Eker and Åström (1996) in order to obtain an estimate of $\dot{\theta}$.

The nonlinear observer has the following structure:

$$\frac{d\hat{x}_1}{dt} = \hat{x}_2 + k_1(x_1 - \hat{x}_1)$$

$$\frac{d\hat{x}_2}{dt} = \omega_0^2 \sin \hat{x}_1 + \omega_0^2 u \cos \hat{x}_1 + k_2(x_1 - \hat{x}_1)$$

where $x_1 = \theta$ and $x_2 = \dot{\theta}$. The design parameters k_1 and k_2 were set to 20 and 60 respectively. The nonlinear observer produced a sufficiently accurate estimate in order to perform successful swing up of the pendulum. (Notice that the measure of θ was used directly for the swing up control law, not the estimate.)

2.4 Friction

On the process used for the experiments friction is a severe complication that can not be neglected. Notice however that it is the friction in the arm (and motor) that is severe, friction in the pendulum pivot point is neglected. The friction gives rise to limit cycles, see Svensson (1998). Friction compensation is therefor highly desirable. We have chosen to use a simple model, Coulomb friction with stiction, which can be written

$$F_f(\dot{\varphi}, u) = \begin{cases} F_c^+ & \dot{\varphi} > 0 \\ F_s^+ & \dot{\varphi} = 0, \quad u > F_c^+ \\ u & \dot{\varphi} = 0, \quad F_s^- < u < F_s^+ \\ F_s^- & \dot{\varphi} = 0, \quad u < F_s^- \\ F_c^- & \dot{\varphi} < 0 \end{cases}$$

The dimension of the friction is angular acceleration, which gives convenient integration with the process model. In the implementation used in the experiments the friction model is simplified further by

$$F_s^+ = F_c^+$$
$$F_s^- = F_c^-$$
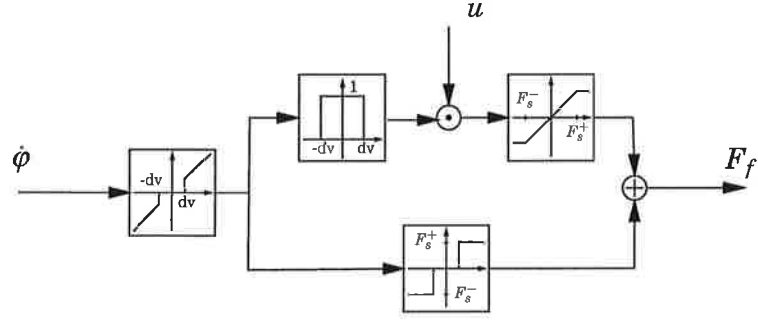
Figure 3 A schematic figure of the Karnopp model.

Estimations of F_c^+ and F_c^- showed that the friction is asymmetric.

Friction compensation is then performed by modifying the control law (4):

$$u = Lx + F_f$$

A practical problem when dealing with the real process is that the measured velocity of the arm is not zero when the arm is at rest, there is a small bias and also measurement noise. To deal with this the Karnopp model presented in Olsson (1996), p. 29 is used. A schematic figure of the model is shown in fig 3. The arm velocity is set to zero if it is within the tolerance limits $\pm$dv. In this case compensation for the stiction effect is performed, otherwise friction compensation corresponding to Coulomb friction is used.

The effect of the friction compensation is significant, the limit cycle is not entirely eliminated, but reduced in amplitude (see fig 4).
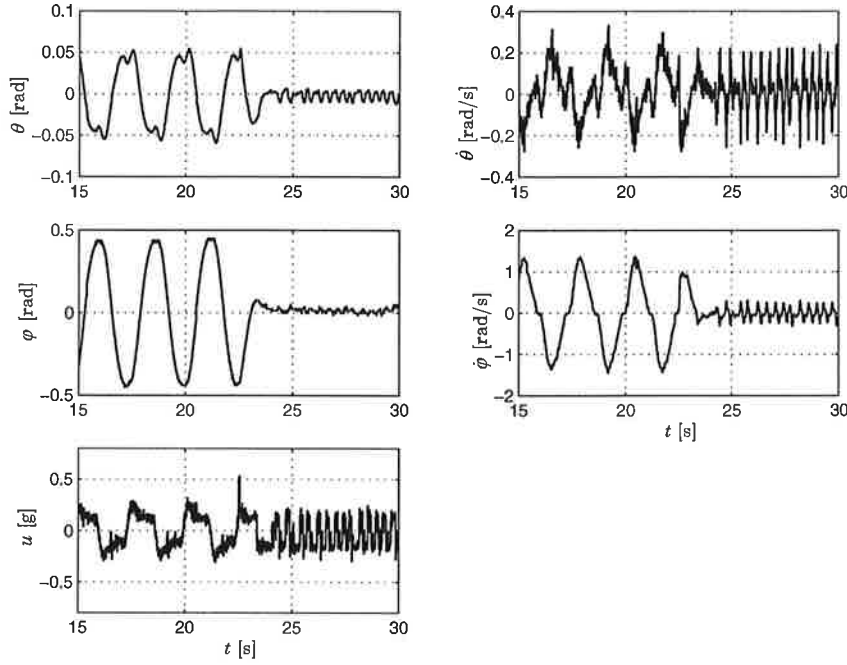
Figure 4 The effect of friction compensation. Notice the significant reduction of the amplitude of the limit cycle for the arm angle.

3. Reference Following with Guaranteed Stability

In this section, a few strategies for implementation of manual control on the inverted pendulum is discussed. A joystick which is connected to the process is used for generation of the control signal. The controlled state is the velocity of the pivot point, i.e $\dot{\varphi}$. An essential condition is that the control of the pivot point must not be performed in such a way that the pendulum cannot be recovered to upright position. Stabilization is considered to be of primary concern.

3.1 A Control law for Velocity Control

When velocity control of the pivot point is performed, it is not a good choice to use the measure of the state φ directly for feedback. Only θ, $\dot{\theta}$ and $\dot{\varphi}$ is used by the state feedback control law. Notice that it would not be acceptable to set the l_3 element in the control law (4) to zero, since the poles of the closed loop system would then not have the desired location. Instead we solve this by deriving a new control law based on a reduced state space model based on only the states θ, $\dot{\theta}$ and φ.

Usage of this reduced control law may result in the pivot point drifting even when the velocity reference is set to zero. To avoid this switching to the control law derived in section 2.2 is performed when the velocity of the pivot point and the velocity reference have both been zero for some short time. (1 s in our implementation.) When the velocity reference deviates from zero, the reduced control law is switched back into use.

12

If the new state space vector

$$\bar{x} = \left(\begin{array}{ccc} \theta & \dot{\theta} & \dot{\varphi} \end{array} \right)^T$$

is is introduced the system (3) may be rewritten as

$$\dot{\bar{x}} = \bar{A}\bar{x} + \bar{B}u = \left(\begin{array}{ccc} 0 & 1 & 0 \\ \frac{\alpha\beta\dot{\varphi}_0^2 + \beta\varepsilon}{\alpha\beta - \gamma^2} & 0 & 0 \\ \frac{-\alpha\gamma\dot{\varphi}_0^2 - \gamma\varepsilon}{\alpha\beta - \gamma^2} & 0 & 0 \end{array} \right) \bar{x} + \left(\begin{array}{c} 0 \\ \frac{-\gamma}{\alpha\beta - \gamma^2} \\ \frac{\alpha}{\alpha\beta - \gamma^2} \end{array} \right) u \qquad (6)$$

Applying the control law

$$u = L\bar{x} \qquad (7)$$

where

$$L = \left(\begin{array}{ccc} l_1 & l_2 & l_3 \end{array} \right)$$

on the system (6) gives a closed loop system with characteristic polynomial

$$s^3 + \frac{\alpha l_3 - \gamma l_2}{\alpha\beta - \gamma^2} s^2 + \frac{-\beta\varepsilon - \alpha\beta\dot{\varphi}_0^2 - \gamma l_1}{\alpha\beta - \gamma^2} s - \frac{(\alpha\dot{\varphi}_0^2 + \varepsilon)l_3}{\alpha\beta - \gamma^2}$$

Let the desired characteristic polynomial of the closed loop system be

$$(s^2 + 2\omega_1\zeta_1 + \omega_1^2)(s + \omega_2)$$

Identification of coefficients gives

$$
\begin{aligned}
l_1 &= -\frac{\alpha\beta\dot{\varphi}_0^2 + \beta\varepsilon}{\gamma} - \frac{\alpha\beta - \gamma^2}{\gamma}(\omega_1^2 + 2\zeta_1\omega_1\omega_2) \\
l_2 &= -\frac{\alpha\beta - \gamma^2}{\gamma}(\frac{2\alpha}{\alpha\dot{\varphi}_0^2 + \varepsilon}\omega_1^2\omega_2 + \omega_2 + \omega_2\zeta_1\omega_1) \\
l_3 &= -\frac{\alpha\beta - \gamma^2}{\alpha\dot{\varphi}_0^2 + \varepsilon}\omega_1^2\omega_2
\end{aligned}
$$

Notice that the feedback vector L is gain scheduled with respect to $\dot{\varphi}$. The numerical values of the design parameters used for the experiments are:

$$\omega_1 = \omega_2 = 14.36$$
$$\zeta_1 = 0.9$$

3.2 Objectives

Before investigating the different methods further the objectives for the control system and a few measures for evaluation is discussed. The meaning of "good control" is usually depending on the process and the demands on the control system. Here we choose to consider two measures of control performance; rise times and state deviations.
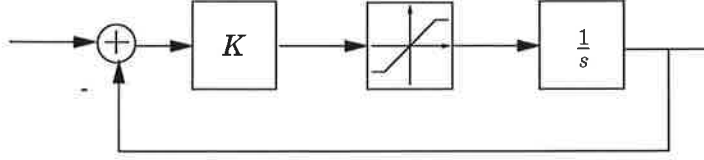
Figure 5 A rate limiter structure.

The rise time for a step is a measure of how fast and well damped the response is. A fast and reasonably well damped response is of course desired. The rise time is here defined as the time from the reference step til the time from which the response stays within given deviations from the reference.

As a measure of the deviations in the states a loss function is introduced as

$$L_l = k_\theta \theta^2 + k_{\dot\theta} \dot\theta^2 + k_{\dot\varphi} \dot\varphi^2$$

where the coefficients is chosen so that the different states get a reasonable weight. The loss function may be considered a measure of the cost in state deviations when control of the pivot point is performed. We have chosen to weight the state errors so that they have about the same influence on the loss function. The following coefficients has been used:

$$k_\theta = 1 \quad k_{\dot\theta} = 0.26 \quad k_{\dot\varphi} = 0.02$$

3.3 A Heuristic Approach

Since the dimension of the reference signal is velocity but the control signal represents an acceleration (the derivative of the velocity), it is reasonable to focus on changes in the reference. Neglecting friction, constant reference signal does not give rise to a control signal, but changes in the reference does. Abrupt changes in the velocity reference may lead to large control signals, possibly saturating, and thereby prevent successful stabilization of the pendulum. This leads us to the idea of using a rate limiter applied on the reference signal to restrict the rate of change in the reference. The rate limiter used here is presented in Rundqwist *et al.* (1997), see fig 5, which provides not only rate limiting, but also a filtering of the reference signal. The parameter K may be used to tune the filtering effect so that the reference gets a little smoothed. This strategy may be implemented so that stability is guaranteed by setting the maximum rate sufficiently low. This would however be a quite conservative method.

A better approach would be to let the limits of the rate limiter be adaptive, i.e. change with the states of the pendulum. It is reasonable to think that the maximum rate of change in the reference, that does not drive the pendulum out of stability, is depending on the states of the pendulum, primarily the pendulum angle and the angular velocity. We introduce

$$\beta = \theta + k\dot\theta$$

where k is chosen so that the weighting between the states is fair. Further, β is used to determine the rates of the rate limiter. A large value of $|\beta|$

14
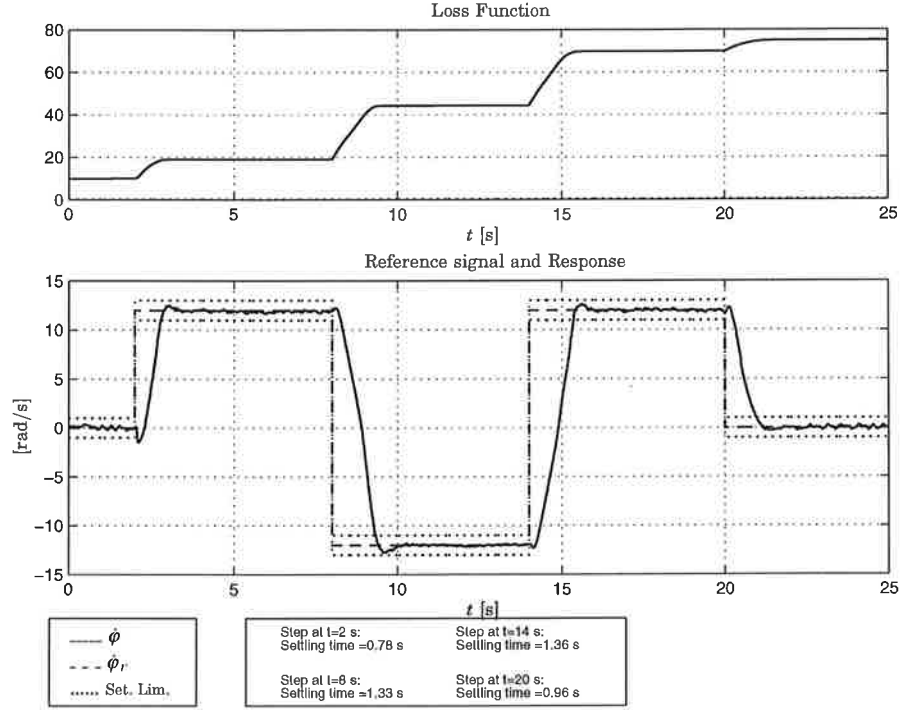
Figure 6 Step responses when using the rate limiter strategy

indicates need of stabilization, the limit should therefore be set tight in this case. On the other hand, small β indicates that the pendulum is not near instability, and faster changes in the reference signal can be allowed.

The mapping from β to the rate limiter limits leaves many possibilities. Here a linear function is used for this purpose,

$$\gamma = k(1 - |\beta|)$$

where γ is the rate limiter limits and k the maximum rate of change. It is here assumed that β is scaled and so that $|\beta| < 1$. This approach gives a result shown in fig 6. Numerical values of the design parameters for this experiment are; β scaling factor is set to 2, and k equals 40.

3.4 The Double Loop Approach

In this section a method described in Brufani (1997) is implemented and evaluated. A few differences may be noted though. In the referenced work a classical inverted pendulum with a linear cart is used for simulations, which differs a bit from the Furta pendulum used by us. Further, Brufani (1997) focuses on position control of the pivot point, not velocity control which is our task. Our experience is that the same basic concepts may be used, but some modifications has to be made in order to achieve good results.

The method presented in Brufani (1997) is based on having two separate control laws for stabilization and reference following respectively. The control law responsible for stabilization should be given high priority so that it keeps the pendulum stable, regardless of the reference signal. The outer loop is allocated the remaining control authority. It should be noticed that
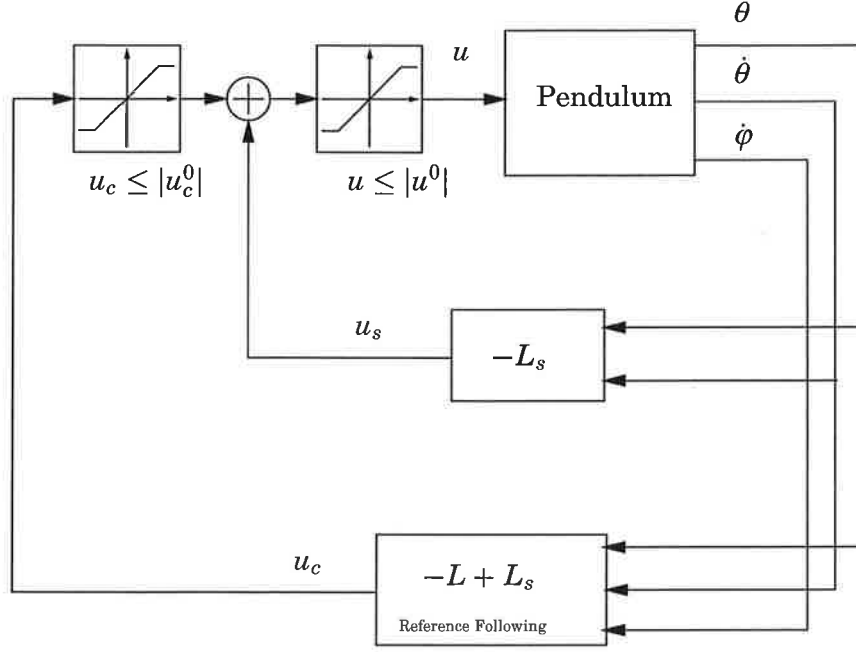
Figure 7 A schematic picture of the double loop strategy. Notice that the state φ is not used for feedback when velocity control is performed.

the inner loop is only used for control when the outer loop is saturating, otherwise it is transparent. A schematic picture of the control structure is given in fig 7. Notice the saturation on the process input which gives rise to the problem. Further, the state feedback vector L_s only uses the states θ and $\dot{\theta}$, while L uses $\dot{\varphi}$ as well. (The state φ is not used when velocity control is performed).

The allocation of control authority is a critical issue as we have argued earlier. In this method this is done by constraining the outer loop with a saturation. Selecting the saturation limits is a key issue.

Stabilization The inner loop should provide stability. Only the states θ and $\dot{\theta}$ is considered for this proposed, that is, the state $\dot{\varphi}$ is neglected. This makes sense since stabilization should be given the highest priority. The control law may be written

$$u_s = L_s \bar{x}$$

where

$$L_s = \left(\begin{array}{cc} l_{s_1} & l_{s_2} \end{array} \right)$$

and

$$\bar{x} = \left(\begin{array}{cc} \theta & \dot{\theta} \end{array} \right)$$

There are several ways to obtain the feedback vector L_s. Since we are also interested in examination of stabilizing regions for the controller, LQ

design is used. This method not only gives us the vector L_s but also a Lyapunov function which may be used for stability analysis. Notice that the vector L_s is gain scheduled with respect to $\dot{\varphi}$.

The process model for the states θ and $\dot{\theta}$ is a reduced version of the state space model (3):

$$\dot{\bar{x}} = \bar{A}\bar{x} + \bar{B}u = \begin{pmatrix} 0 & 1 \\ \frac{\alpha\beta\dot{\varphi}_0^2 + \beta\varepsilon}{\alpha\beta - \gamma^2} & 0 \end{pmatrix} \bar{x} + \begin{pmatrix} 0 \\ \frac{-\gamma}{\alpha\beta - \gamma^2} \end{pmatrix} u \qquad (8)$$

LQ theory give the linear controller that minimizes the loss function

$$J = \int_0^\infty \bar{x}^T Q \bar{x} + u^T R u \, dt$$

where Q and R are positive definite symmetric matrices. These are the tuning knobs used to obtain desired behavior. The optimal controller is given by

$$L_s = R^{-1}B^T S$$

where S is the matrix that solves the steady state Riccati equation

$$A^T S + SA + Q - SBR^{-1}B^T S = 0$$

The matrix S can also be used to form a Lyapunov function:

$$V(\bar{x}) = \bar{x}^T S \bar{x}$$

The Lyapunov theory specifies three condition for Lyapunov stability:

1. $V(\bar{x}) = 0, \quad \bar{x} = 0$
2. $V(\bar{x}) > 0, \quad \bar{x} \neq 0$
3. $\dot{V}(\bar{x}) < 0$

It is obvious that the first condition is satisfied. The second i satisfied since S is positive definite. It remains to examine the region where the derivative of the Lyapunov function is negative; this gives us the region in which the control law stabilizes the system. However this Lyapunov function is valid for the linearized system, but not necessarily for the real system.

In the experiments the design parameters for the LQ design have been chosen as:

$$R = 0.20 \quad Q = \begin{pmatrix} 96.98 & 17.10 \\ 17.10 & 3.03 \end{pmatrix}$$

Velocity control of the pivot point   The control law responsible for velocity control is the outer loop in fig 7. The feedback vector L is identical with the one calculated in section 2.2. The vector L_s (L_s is actually extended with two zeros for the states φ and $\dot{\varphi}$ in order to get the correct size) is added to L to make the inner stabilizing control law transparent when the outer loop is not saturating.

To summarize the characteristics of the controller, a few different modes of operation may be recognized.

$$
\begin{array}{llll}
\Omega_0 & u = -l_1\theta - l_2\dot{\theta} - l_4\dot{\varphi} & |u_c + u_s| \leq u^0 & |u_c| \leq u_c^0 \\
\Omega_1^+ & u = u_c^0 - l_{s1}\theta - l_{s2}\dot{\theta} & |u_s + u_c| \leq u^0 & u_c \geq u_c^0 \\
\Omega_1^- & u = -u_c^0 - l_{s1}\theta - l_{s2}\dot{\theta} & |u_s - u_c| \leq u^0 & u_c \leq -u_c^0 \\
\Omega_2^+ & u = u^0 & u_s + u_c^0 \geq u^0 & \\
\Omega_2^- & u = -u^0 & u_s + u_c^0 \leq -u^0 &
\end{array}
$$

When in mode Ω_0 the system is controlled by the control calculated in section 2.2. This control law takes changes in the reference signal into account; it is responsible for the reference following.

In the next two modes, Ω_1^+ and Ω_1^- the outer control law is saturated. This means that the inner loop is in action, stabilizing the system. Notice however that a constant contribution (i.e the saturation limit of the outer loop) is added to the control law.

In the last two modes of operation, Ω_2 and Ω_2, the inner control loop is saturated. This desirable to avoid this modes, stability is likely to be lost in this region of operation.

So far the saturation limits of the outer loop has been considered fixed. An attractive idea would be to let these limits depend on θ and $\dot{\theta}$. When the pendulum is in fairly upright position the limits may be set wide apart, but if the pendulum approaches instability the limits should be set tight in order to guarantee sufficient control authority for the inner stabilizing loop. As measure of the stability of the pendulum we choose to consider the momentary energy stored in the pendulum. An expression of the energy similar to that presented in 2.3 is used here.

$$
E_n = \frac{\dot{\theta}^2}{2\omega_0^2}sign(\dot{\theta}) + (\cos\theta - 1)sign(\theta)
$$

Notice however that the signs of θ and $\dot{\theta}$ is also considered. Not only the magnitude of the energy is important but also the sign of the angle and the direction of the angular velocity have to influence the choice of saturation limits for the outer loop.

The mapping from the energy E_n to the saturation limits may be implemented in many ways. We will choose a quite simple method, and may thereby not take full advantage of the concept.

Firstly we have experienced that it is desirable to low pass filter the energy estimation. If the value of the energy was allowed to directly affect the saturation limits, a chattering effect appeared which cannot be accepted.
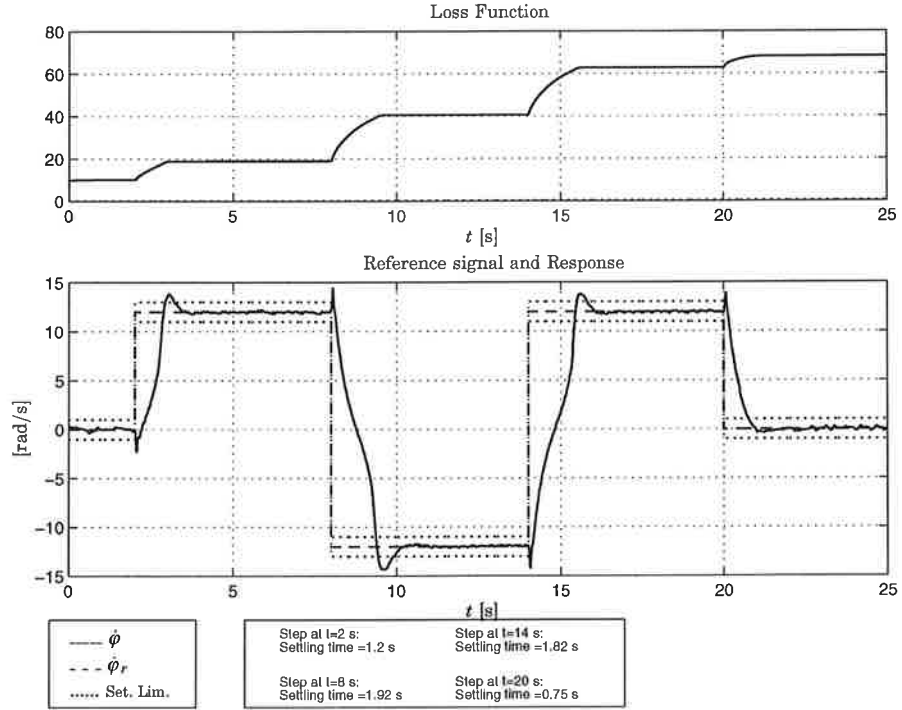
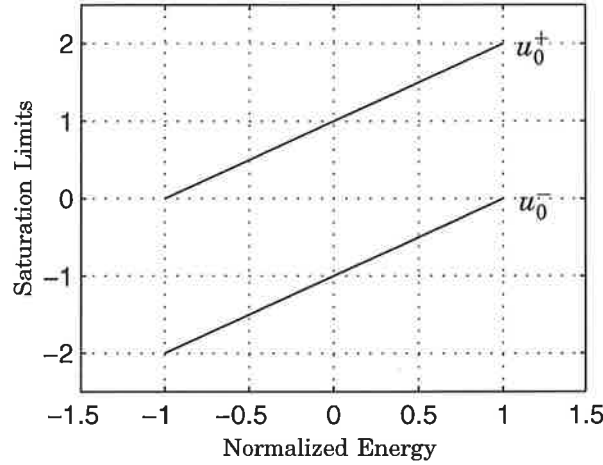**Figure 8** Step responses for the double loop strategy. Fixed saturation limits, ±1.5 is used.

A Bessel filter with a bandwidth of 4 rad/s was used for this purpose. Further, the energy is normalized so that $|E_n| \leq 1$. In order to get a good coverage of the interval [-1 1] E_n should be scaled, we have used a scaling factor of 70 for the experiments.

The mapping from the normalized energy to the saturation limits is illustrated in fig 9. The saturation limits are asymmetric; high positive energy (e.g positive angle and positive angular velocity) means that large positive reference changes may be made, while negative reference changes gets little response.

The design parameter of this mapping is the slope of the saturation lines. In fig 9 the slope is set to 1, but in our experiments the value 2.5 is used. Low values of the slope indicates tight saturation limits and thereby a restrictive strategy. Larger values may give faster control strategies, but it is then possible that the guaranteed stability is lost. Hence, the choice of saturation limits is a tradeoff between fast control and robustness. An experiment showing a step sequence and the $\dot{\varphi}$ response when the adaptive saturation limits strategy is may be seen in fig 10.

3.5 Results

Two different strategies (and two different versions of the later) have been implemented and evaluated in this section. The results can be seen in the figures 6, 8 and 10. Comparing these plots, the rate limiter seems to be superior. This strategy is both faster and better damped than the ones based on the double loop strategy. This however, does not necessarily mean that this method is superior compared to the other. A few reasons for this may be recognized. Firstly, the rate limiter strategy is fairly easy to tune

Figure 9 Mapping of saturation limits for the outer control loop from normalized energy.
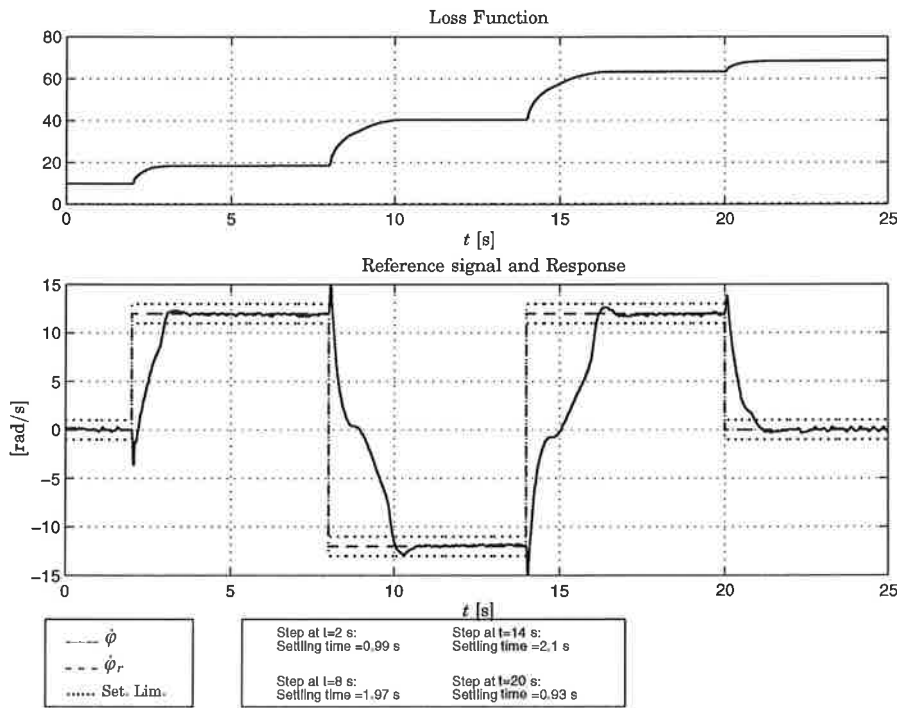
Figure 10 Step responses for the double loop strategy. The limits of the saturation for the outer loop are here adaptive.

for optimal performance, quite few design parameters have to be decided. The double loop strategy contains numerous design choices; the LQ design, choice saturation limits etc.

Further, the analysis of the double loop strategy may be extended in order to gain improved understanding, and thereby probably improved performance. The concept of adaptive saturation limits for the outer loop (i.e. adaptive allocation of control authority) is discussed only briefly in this work, and it is likely that significant improvements can be made here. The

analysis of these issues, however, is left for future research.

4. Implementation

So far all calculations have been done in continues time. The experiments however have been performed using discrete controllers implemented on a computer. This approximation should not affect the validity of the results, since a short sampling period, 10 ms, has been used. Matlab has been used for calculations of the discrete controllers.

4.1 Experimental Set Up

A Furuta pendulum, a joystick and a personal computer were used for the experiments. This section describes the set up; connections etc.

The Pendulum   The pendulum used for the experiments provides several measured signals; arm position and velocity, pendulum angle and angular velocity. The later signals exist in two separate versions, one that covers all possible pendulum angles and one that only covers angles near the upright position. The top angle measurements were used for stabilization and velocity control, while the the full lap signals were used for the swing up sequence.

The signals from the pendulum were connected to the I/O interface on the computer in the following way:

I/O Connection	Pendulum Signal
AI2	Pendulum Angle (Top)
AI3	Pendulum Velocity (Top)
AI4	Arm Position
AI5	Arm Velocity
AI6	Pendulum Angle (360°)
AI7	Pendulum Velecity (360°)
AO0	Control signal
Ground	Ground

The Joystick   A joystick connected to the computer offers a quite good reference generator when to demonstrate manual control, but for the experiments computer generated reference signals were used in order to enable fair comparison between the different strategies. The joystick signal (only the X axis signal was used) represents the desired velocity of the pivot point. For power supply a DC servo were used. Connections were made as follows:

I/O Connection	Joystick Signal
AI0	White (X Axis)
AI1	Blue (Y Axis)
DC Servo, +9V	Red
DC Servo, Ground	Black

The Computer A PC, 166 MHz Pentium, running Linux as operating system and an I/O interface connected to it were used. For all simulations and experiments Matlab 5.2 in combination with Simulink were used.

4.2 The Simulink Interface

All control structures has been calculated using Matlab and implemented in Simulink. Simulink in combination with the I/O interface (the interface with the hardware I/O implemented as S-functions, see [Anders Blomdell]) offers the possibility to easily evaluate controllers by simulation before performing the experiment on the real pendulum.

A few practical advices are worth mentioning to ease the procedure of reconnecting the pendulum reprocducing a well functioning demonstration.

Firstly, it is critical to make sure that the measured signals are transformed from Volts to rad, rad/s etc in a proper way. This is done by examining the signals in the block *Process/Hardware/Conversion of Inputs*. Especially it is critical to make sure that the measurements of the θ angle is zero when the pendulum is in upright position.

Further it is possible that the tracking coefficients has to be adjusted, in order to achieve accurate static reference following. This is done by modifying the blocks *Controller / Reference/Conroller/Johan Heuristic/Tracking* and *Controller / Reference/Conroller/Double Loop/Tracking* respectively.

4.3 Experienced Problems

In this section some of the practical problems experienced during the project will be discussed.

A major problem at the beginning of the project was measurement noise. Although stabilization of the pendulum was possible, it was hard to distinguish the signals, (this problem was most serious for the angular velocity of the pendulum) because of noise. The most significant reason for this was that the pendulum and the computer were connected to power supplies with common ground point far from the plugs. This caused a long ground loop which received a lot of noise. The problem was significantly reduced when pendulum and computer were connected to plugs close to each other. Shielded cables were used for the measured signal with the most severe noise and the control signal. This reduced the noise further. The remaining noise was found to be acceptable.

A problem that appeared right after the swing up sequence finished was a high frequent oscillation in the pendulum. High frequent is here meant to be compared to the natural frequency of the pendulum. Since the frequency of this occillation was higher than the bandwidth of the closed loop system it could not be damped by the control law. Our solution to the problem was to simply damp the occillation manually.

A problem experienced in Simulink is worth to mention. The original idea was to include both a model of the pendulum and the hardware interface in the same structure, enabling fast and easy switching between simulation and experiment. However, this turned out to be a problem since the continous states of the model required to much calculation time when experiment were performed on the real pendulum. It was not possible to

keep up the sampling rate which was unacceptable. The solution was to remove the pendulum model during the experiments and insert it for the simulations.

A phenomena that grew more and more significant durig the project were periodic spikes in the "jitter" curve. The measured signals exabited more or less significant discontinousies at those times. This problem caused a lot of confusion, but was tracked down to depend on the numerous Scopes used in the application for debugging purposes. When the Scope buffers were updated every fifth second, the sampling time could not be held. The problem was solved by removing the scopes from the application.
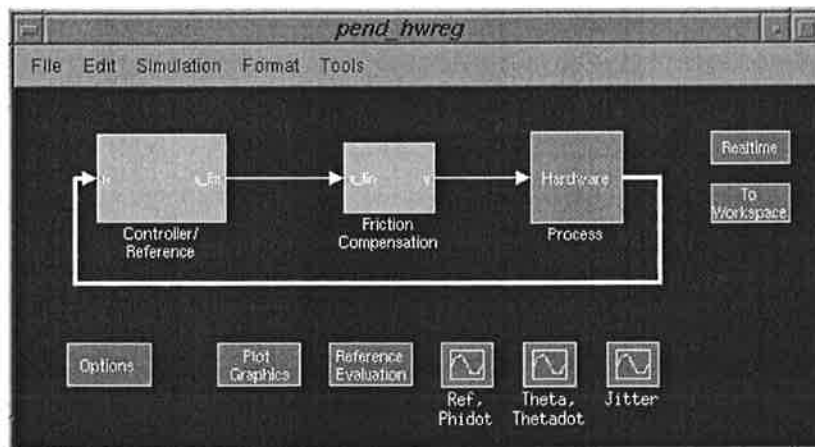
Figure 11 The main view of the user interface.

A. User Interface

The main view of the user interface is seen in fig 11. All relevant plots and controls should be located in this view. To start the demonstration, make sure the pendulum is at rest (either hanging down or standing upright) and press *Ctrl+t*. If the pendulum was at rest hanging down, the swing up sequence is started by moving the joystick in any direction along the x-axis. When the pendulum has reached its upright position the velocity of the pendulum can be controlled.

A few buttons appear in the main view, their function is explained by the following table:

Button	Function
Options	The application may be set to operate in two modes, either open loop or closed loop. Closed loop is normally used, but open loop may be used for debug purposes. In the later case no control signal is given to the process, but all measured signals are logged. Further, two ways of generating reference the signal is allowed. Either the joystick or a sequence of reference steps. It is possible to change the step sequence by modifying the block *Controller/Reference / Controller / Reference generator*. Finally, any of the implemented strategies may be selected.
Plot Graphics	Displays a plot showing θ, $\dot{\theta}$, φ, $\dot{\varphi}$, u and jitter
Reference Evaluation	Displays the loss function as well as the reference signal and response. Also calculates rise times. (Works best when the step sequence is used.)
Ref, $\dot{\varphi}$	A real time plot showing the reference and phidot.
θ, $\dot{\theta}$	A real time plot showing θ and $\dot{\theta}$.
Jitter	A real time plot of the jitter.

Both control of the real pendulum and simulation using a model is possible. However the pendulum model is not included when control of the real pendulum is performed. If it was, the sampling rate may not be kept since the continous states of the model takes too much calculation time. Instead the model has to be imported before simulations can be done. The model is stored in the file *pend_model.mdl* and should be imported to the block *Process*. Double click the block *Process* to enable the simulation.

B. References

Åström, K. J. and K. Furuta (1999): "Swinging up a pendulum by energy control." *Automatica*. To be published.

Brufani, S. (1997): "Manual control of unstable systems." Master thesis ISRN LUTFD2/TFRT--5576--SE. Department of Automatic Control, Lund Institute of Technology, Lund, Sweden.

Canudas de Vit, C., K. J. Åström, and K. Braun (1987): "Adaptive friction compensation in DC-motor drives." *IEEE Trans. Robotics and Automation*, **RA-3**, pp. 681–685.

Eker, J. and K. J. Åström (1996): "A nonlinear observer for the inverted pendulum." In *Proc. IEEE Conference on Control Applications*, pp. 332–337. Dearborn, Michigan.

Gäfvert, M. (1998): "Derivation of furuta pendulum dynamics." Technical Report. Department of Automatic Control, Lund Institute of Technology, Lund, Sweden.

Olsson, H. (1996): *Control Systems with Friction.* PhD thesis ISRN LUTFD2/TFRT--1045--SE, Department of Automatic Control, Lund Institute of Technology, Lund, Sweden.

Patcher, M. and M. R.B. (1998): "Manual flight control with saturating actuators." *IEEE Control Systems*, February, pp. pp. 10–19.

Rundqwist, L., S.-G. K., and J. Enhagen (1997): "Rate limiters with phase compensation in jas 39 gripen." In *Proc. European Control Conference.* Saab Military Aircraft, Linköping, Sweden.

Svensson, J. (1998): "Effects of friction on the Furuta pendulum." Master thesis ISRN LUTFD2/TFRT--5593--SE. Department of Automatic Control, Lund Institute of Technology, Lund, Sweden.